I&EC research
Industrial & Engineering Chemistry Research

pubs.acs.org/IECR

Article

Computational Investigation of Dual Filler-Incorporated Polymer Membranes for Efficient CO_2 and H_2 Separation: MOF/COF/Polymer Mixed Matrix Membranes

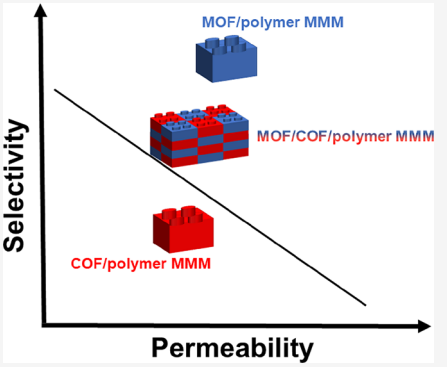
Sena Aydin, Cigdem Altintas, Ilknur Erucar, and Seda Keskin*

Cite This: *Ind. Eng. Chem. Res.* 2023, 62, 2924−2936

Read Online

ACCESS | Metrics & More | Article Recommendations | Supporting Information

ABSTRACT: Mixed matrix membranes (MMMs) composed of two different fillers such as metal−organic frameworks (MOFs) and covalent−organic frameworks (COFs) embedded into polymers provide enhanced gas separation performance. Since it is not possible to experimentally consider all possible combinations of MOFs, COFs, and polymers, developing computational methods is urgent to identify the best performing MOF−COF pairs to be used as dual fillers in polymer membranes for target gas separations. With this motivation, we combined molecular simulations of gas adsorption and diffusion in MOFs and COFs with theoretical permeation models to calculate H_2, N_2, CH_4, and CO_2 permeabilities of almost a million types of MOF/COF/polymer MMMs. We focused on COF/polymer MMMs located below the upper bound due to their low gas selectivity for five industrially important gas separations, CO_2/N_2, CO_2/CH_4, H_2/N_2, H_2/CH_4, and H_2/CO_2. We further investigated whether these MMMs could exceed the upper bound when a second type of filler, a MOF, was introduced into the polymer. Many MOF/COF/polymer MMMs were found to exceed the upper bounds showing the promise of using two different fillers in polymers. Results showed that for polymers having a relatively high gas permeability ($\geq 10^4$ barrer) but low selectivity (≤ 2.5) such as PTMSP, addition of the MOF as the second filler can have a dramatic effect on the final gas permeability and selectivity of the MMM. Property−performance relations were analyzed to understand how the structural and chemical properties of the fillers affect the permeability of the resulting MMMs, and MOFs having Zn, Cu, and Cd metals were found to lead to the highest increase in gas permeability of MMMs. This work highlights the significant potential of using COF and MOF fillers in MMMs to achieve better gas separation performances than MMMs with one type of filler, especially for H_2 purification and CO_2 capture applications.



Downloaded via KOC UNIV on December 30, 2023 at 11:34:22 (UTC).
See https://pubs.acs.org/sharingguidelines for options on how to legitimately share published articles.

1. INTRODUCTION

Membrane-based gas separation is an effective technology to capture carbon dioxide from natural gas and flue gas, to purify hydrogen and olefins from nitrogen, to dehumidify air and natural gas, and to separate different hydrocarbon pairs including alkanes/alkenes under easy-to-operate and energy-efficient conditions.[1] Polymeric membranes suffer from a well-known gas permeability−selectivity trade-off as highlighted by Robeson;[2−4] therefore, current membrane research is focused on the discovery of new membrane materials with enhanced gas permeability and selectivity properties to surpass the upper bound of polymeric membranes.[5−7] Mixed matrix membranes (MMMs), which consist of a polymer incorporated with an organic/inorganic porous filler, offer enhanced gas separation performances through the combination of easy processability of polymers with high gas permeability/selectivity of fillers such as zeolites, graphene oxides, carbon molecular sieves, metal−organic frameworks (MOFs), and covalent−organic frameworks (COFs).[8−11] These MMMs have been used for many important gas separations such as H_2 purification and air purification.[12]

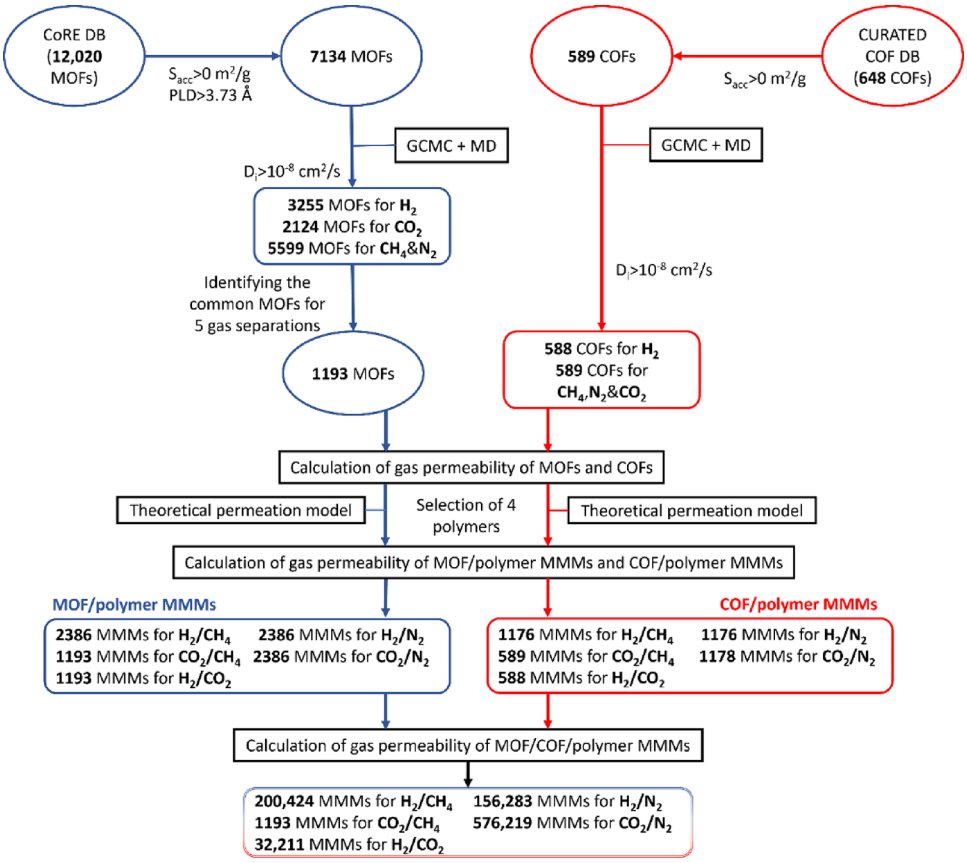
The metal nodes and organic linkers that make up MOFs are connected in a variety of topologies, providing vast space for structural tunability, with a wide range of surface areas, well-defined pore size distributions, and high porosity.[13] COFs generally consist of B, C, O, N, and Si elements covalently linked to organic linkers.[14] The structural and chemical diversity of MOFs is currently represented with more than 110,000 MOFs available in the Cambridge Structural Database,[15] while the most recent COF database now includes more than 700 synthesized COFs.[16] Both experimental and computational studies showed that many MOF and COF membranes can exhibit high gas permeabilities.[17,18] Synthesis of thin-film membranes from crystalline materials is challenging due to many issues such as poor interactions with the

Received: December 13, 2022
Revised: January 12, 2023
Accepted: January 16, 2023
Published: January 26, 2023



© 2023 The Authors. Published by American Chemical Society

Scheme 1. Computational Approach of This Work Combining Molecular Simulations of MOFs and COFs with Theoretical Permeation Models to Predict H_2, N_2, CH_4, and CO_2 Permeabilities of MOF/COF/Polymer MMMs



substrates, crack formation, and moisture instability, which affect the practical implementation and scalability of thin-film MOF and COF membranes.[19] Therefore, MOFs and COFs have been recently used as filler particles in polymers to make MMMs.[20] Incorporation of MOFs as fillers into polymers has led to many MOF/polymer MMMs, which offer higher gas permeability and/or selectivity than the pure polymer membrane, but these MMMs generally suffer from compatibility issues between MOFs and polymers due to the inorganic nature of MOFs.[21] On the other hand, COFs offer better interfacial compatibility with polymers compared to MOFs thanks to the completely organic structure of COFs.[21] COFs generally have larger pore sizes than MOFs, which offer high gas permeability but limited selectivity since both gas molecules can pass through these large pores.[22]

Generating MMMs having both high gas permeability and high selectivity can be possible using dual types of fillers via combining two types of porous materials with a polymer. In the first experimental report on the dual filler-incorporated MMMs, Zornoza et al.[23] examined MMMs where a MOF (HKUST-1 or ZIF-8) and a zeolite (S1C) were incorporated into polysulfone (PSF) to generate HKUST-1/S1C/PSF and ZIF-8/S1C/PSF MMMs and tested them for separation of equimolar CO_2/CH_4, CO_2/N_2, O_2/N_2, and H_2/CH_4 mixtures. The highest CO_2/CH_4 and CO_2/N_2 selectivities (22.4 and 38, respectively) were attained with the HKUST-1/S1C/PSF MMM, whereas selectivities of single filler-incorporated MMMs, HKUST-1/PSF MMM (15.8 and 22.9, respectively) and ZIF-8/PSF MMM (19.3 and 19.8, respectively), were found to be lower at 2.75 bar and 308 K. HKUST-1/S1C/PSF MMMs showed higher O_2 permeabilities and O_2/N_2 selectivities (1.7 Barrer and 8.1, respectively) than the single filler-incorporated HKUST-1/PSF MMM (2.2 Barrer and 5.1, respectively).

Two different MOFs, MIL-101(Cr) and ZIF-8, were incorporated into PSF and CO_2/CH_4 separation performances of MMMs were tested at 2 bar and 308 K.[24] The selectivity of MIL-101(Cr)/ZIF-8/PSF MMM (40) was reported to be higher than the selectivities of MMMs having a single filler, MIL-101(Cr)/PSF MMM (24) and ZIF-8/PSF MMM (22), and the neat polymer (23). In addition to the high CO_2/CH_4 selectivity, CO_2 permeability of MIL-101(Cr)/ZIF-8/PSF MMM (14.2 Barrer) was higher than the CO_2 permeabilities of the MIL-101(Cr)/PSF MMM (8.9 Barrer), ZIF-8/PSF MMM (13.7 Barrer), and PSF membrane (4.7 Barrer). CuBDC and ZIF-8 were incorporated into the pure ODTA-TMPDA polymer to study the separation of an equimolar CO_2/CH_4 mixture at 1 bar and 298 K.[25] ZIF-8/CuBDC/ODTA-TMPDA MMMs with different ZIF-8 and CuBDC filler loadings showed improved CO_2 permeability compared to the pure ODTA-TMPDA membrane, and the highest CO_2/CH_4 selectivity (47) was obtained with the ZIF-8/CuBDC/ODTA-TMPDA MMM compared to the selectivities of the ODTA-TMPDA, ZIF-8/ODTA-TMPDA MMM, and CuBDC/ODTA-TMPDA MMM (36, 37, and 43 respectively).

As this literature summary suggests, there is a significant potential in utilizing dual types of fillers in MMMs to achieve higher gas permeabilities and selectivities compared to those offered by MMMs having a single type of filler. Examining gas

https://doi.org/10.1021/acs.iecr.2c04500
Ind. Eng. Chem. Res. 2023, 62, 2924−2936

separation performances of MMMs having various combinations of MOFs and COFs as dual fillers is required to unlock the full potential of MOF/COF/polymer MMMs for different gas separations. In this work, we aimed to predict gas separation performances of MOF/COF/polymer MMMs and to identify the best performing MOF/COF/polymer MMMs for H_2 and CO_2 separations. Considering the very large number of existing MOFs, COFs, and polymers, it is not possible to experimentally test every single combination of MOF/COF/polymer MMMs for a target gas separation. Motivated by this, we introduced a computational approach based on molecular simulations and theoretical gas permeation models to predict gas permeabilities and selectivities of almost a million different types of MOF/COF/polymer MMMs. We studied 966,330 MMMs obtained from the combination of 1193 MOFs, 589 COFs, and 4 different polymers, which represent the largest number and variety of MOF/COF/polymer MMMs examined to date. Permeabilities and selectivities of these MOF/COF/polymer MMMs have been studied for 5 important gas separations: H_2/N_2, H_2/CH_4, H_2/CO_2, CO_2/N_2, and CO_2/CH_4. Using the very large amount of membrane performance data produced by molecular simulations and permeation models, we analyzed structure−performance relations to understand how the structural properties of MOFs and COFs affect the permeability and selectivity of the resulting MOF/COF/polymer MMMs. Results of this work will provide significant insights into identifying the most useful MOF/COF pairs that can be utilized as dual fillers in polymer membranes and accelerate the design and development of the ideal MOF/COF/polymer MMMs for H_2 purification and CO_2 capture applications.

2. COMPUTATIONAL METHODOLOGIES

We designed a computational approach combining molecular simulations of gas adsorption and diffusion in MOFs and COFs together with the theoretical permeation models to calculate H_2, N_2, CH_4, and CO_2 permeabilities of MOF/COF/polymer MMMs as shown in Scheme 1. We initially considered 12,020 MOFs taken from the most recent computation-ready, experimental (CoRE) MOF database[26] and 648 COFs taken from the Clean, Uniform, and Refined with Automatic Tracking from Experimental Database (CURATED)[16] as fillers for MMMs. Structural properties of MOFs and COFs such as the largest cavity diameter (LCD), pore limiting diameter (PLD), accessible surface area (S_{acc}), and porosity were computed via Zeo++ software.[27] We used a probe radius of 1.86 Å representing the radius of N_2 to predict S_{acc} of MOFs and COFs and only focused on materials with PLD > 3.73 Å and S_{acc} > 0 m^2/g to be able to compute gas permeability. Adsorption amounts of H_2, N_2, CH_4, and CO_2 (H_2, N_2, and CH_4) in MOFs (COFs) were calculated using grand canonical Monte Carlo (GCMC) simulations at 1 bar and 298 K, and molecular dynamics (MD) simulations were performed at the adsorbed gas loadings to compute self-diffusivities of gases in MOFs and COFs as described in detail in our previous studies.[22,28] To obtain statistically accurate data from MD simulations, we discarded the MOFs and COFs for which self-diffusion coefficients of gases were computed to be less than 10^{-8} cm^2/s. After this refinement, we ended up with 2124, 3255, 5599, and 5599 MOFs for which CO_2, H_2, CH_4, and N_2 adsorption and diffusion data were generated by molecular simulations.[28] Since we aimed to study five different gas separations, H_2/N_2, H_2/CH_4, H_2/CO_2, CO_2/N_2, and CO_2/CH_4, we focused on the 1193 common MOFs for which these data are available for all four gases.

We previously reported H_2 (N_2 and CH_4) adsorption and diffusion data at 1 bar and 298 K for 588 (589) COFs using molecular simulations.[22] Additionally, we performed GCMC and MD simulations for CO_2 in this work using RASPA software (version 2.0.35)[29] and obtained CO_2 uptakes and self-diffusion coefficients in COFs at 1 bar and 298 K. Lennard-Jones 12-6 (LJ) and Coulomb potentials were used to describe dispersion and electrostatic interactions, respectively. CO_2 was modeled as a linear and three-site rigid molecule, and electrostatic interactions between COF and CO_2 molecules were considered.[30] The LJ parameters of atoms in COFs were acquired from the universal force field (UFF),[31] and these atoms were already assigned with the density-derived electrostatic and chemical (DDEC) charges.[16] The details of simulation parameters and conditions can be found in Table S1.

After adsorption and diffusion data of gases in MOFs and COFs were obtained from GCMC and MD simulations, permeabilities of MOFs and COFs for gas species i (P_i^{MOF} and P_i^{COF}) were calculated as shown in eqs 1 and 2 using the adsorbed concentration of gas i (c_i), the self-diffusion coefficient of gas i (D_i), and the feed side pressure of the membrane (f) at 1 bar. The permeate side of the membrane was assumed to be at vacuum:[32]

$$P_i^{MOF} = c_i^{MOF} D_i^{MOF} / f \tag{1}$$

$$P_i^{COF} = c_i^{COF} D_i^{COF} / f \tag{2}$$

We then used a theoretical permeation model, the Maxwell model,[33,34] to compute the gas permeabilities of MMMs having a single type of filler. All permeability data were obtained for 1 bar and 298 K. Permeabilities of MOF/polymer MMMs ($P_i^{MOF/polymer\ MMM}$) and COF/polymer MMMs ($P_i^{COF/polymer\ MMM}$) were calculated as follows:

$$P_i^{MOF/polymer\ MMM} = P_i^{P}\left[\frac{2(1-\phi) + (1+2\phi)(\lambda_{MOF/polymer})}{(2+\phi) + (1-\phi)(\lambda_{MOF/polymer})}\right] \tag{3}$$

$$P_i^{COF/polymer\ MMM} = P_i^{P}\left[\frac{2(1-\phi) + (1+2\phi)(\lambda_{COF/polymer})}{(2+\phi) + (1-\phi)(\lambda_{COF/polymer})}\right] \tag{4}$$

in which P_i^P is the gas permeability of the neat polymer for gas species i that we obtained from the literature (listed in Table S2), $\lambda_{MOF/polymer} = P_i^{MOF}/P_i^P$, $\lambda_{COF/polymer} = P_i^{COF}/P_i^P$, and ϕ describes the volume fraction of the filler (either the MOF or COF) in the polymer matrix. The Maxwell model is one of the most commonly used theoretical permeation models and known to be valid at low filler loadings ($\phi \leq 0.2$).[33] Thus, the volume fraction of the filler was set to 0.2. Selectivities of MOF/polymer MMMs and COF/polymer MMMs for gas species i over j were computed as the ratio of the corresponding gas permeabilities as follows:

$$S_{i/j}^{MOF/polymer\ MMM} = P_i^{MOF/polymer\ MMM} / P_j^{MOF/polymer\ MMM} \tag{5}$$

$$S_{i/j}^{COF/polymer\ MMM} = P_i^{COF/polymer\ MMM} / P_j^{COF/polymer\ MMM} \tag{6}$$

https://doi.org/10.1021/acs.iecr.2c04500
Ind. Eng. Chem. Res. 2023, 62, 2924−2936

We specifically focused on 4 different polymers, PTMSP, PTMSP-co(95/5), Teflon AF-2400, and PIM-1[35−37] for 5 different gas separations studied in this work. We selected PTMSP, PTMSP-co(95/5), Teflon AF-2400, and PIM-1 among the polymers which define the Robeson's upper bound for each gas separation. PTMSP and PIM-1 were studied for CO_2/N_2 separation since PTMSP has a high CO_2 permeability and PIM-1 offers a relatively high CO_2/N_2 selectivity. For CO_2/CH_4, we focused on a highly selective polymer PIM-1. For H_2/N_2, H_2/CH_4, and H_2/CO_2 separations, we studied PTMSP-co(95/5) since it has a high H_2 permeability. Teflon AF-2400 and PIM-1 were studied for H_2/CH_4 and H_2/N_2 separations due to their relatively high selectivity. Experimental gas permeabilities and selectivities of these polymers were collected from the literature and are listed in Table S2. As a result, we focused on 2386 MOF/polymer MMMs and 589 COF/polymer MMMs for CO_2/N_2 separation, 1193 MOF/polymer MMMs and 589 COF/polymer MMMs for CO_2/CH_4 separation, 2386 MOF/polymer MMMs and 1176 COF/polymer MMMs for H_2/CH_4 separation, 2386 MOF/polymer MMMs and 1176 COF/polymer MMMs for H_2/N_2 separation, and 1193 MOF/polymer MMMs and 1176 COF/polymer MMMs for H_2/CO_2 separation.

After calculating the gas permeability and selectivity of MOF/polymer MMMs and COF/polymer MMMs, we identified 1193 common MOF/polymer MMMs and 589 COF/polymer MMMs for H_2/N_2, H_2/CH_4, CO_2/N_2, CO_2/CH_4, and H_2/CO_2 separations. To compute the gas permeability of MOF/COF/polymer MMMs for gas species i ($P_i^{\text{MOF/COF/polymer MMM}}$), we used an approximate model, which was previously defined to express the permeability in binary blends of polymers and copolymers:[38]

$$\log P_i^{\text{MOF/COF/polymer MMM}} = \phi_1 \log P_i^{\text{MOF/polymer MMM}} + \phi_2 \log P_i^{\text{COF/polymer MMM}} \quad (7)$$

Here, ϕ_1 and ϕ_2 represent the filler volume fractions of the MOF/polymer MMM and the COF/polymer MMM in the MOF/COF/polymer MMM. They were used as 0.5 to assume that equal volumes of MOF/polymer and COF/polymer MMMs are utilized to obtain the MOF/COF/polymer MMM. The validity of this approximate model was previously shown by comparing its predictions for CO_2, N_2, and CH_4 permeabilities of the ZIF-8/S1C/PSF MMM and CuBTC/S1C/PSF MMM with the experimental measurements.[39] In this work, we also calculated H_2, N_2, O_2, CO_2, and CH_4 permeabilities of MOF/S1C/PSF MMMs using molecular simulations and eq 7 for two different MOFs (ZIF-8 and CuBTC) at the same conditions with the experiments reported in the literature. Gas permeabilities of two MOFs were calculated in this work, while data for S1C and PSF were taken from the literature.[23] Figure S1 shows that there is good agreement between the calculated and experimental permeabilities of ZIF-8/S1C/PSF MMMs and HKUST/S1C/PSF MMMs for H_2, N_2, O_2, CO_2, and CH_4, demonstrating the validity of our approach for assessing separation performances of dual filler-incorporated MMMs.

It was recently shown that MOFs generally have higher selectivities compared to COFs in membrane-based gas separation applications.[22] Thus, we specifically focused on COF/polymer MMMs located below the upper bound due to their low selectivity for 5 different gas separations in this work and explored if they can exceed the upper bound when a second type of filler, a MOF, is introduced into the polymer. The numbers of all COF/polymer MMMs located below the upper bound and used to generate MOF/COF/polymer MMMs for each separation are given in Table S3. To quantify the improvements of using dual fillers (a MOF and a COF) instead of using only a COF filler in MMMs, we defined the percent (%) changes in gas permeabilities and selectivities of MOF/COF/polymer MMMs, which are located above the upper bound with respect to the gas separation performances of COF/polymer MMMs. The percent changes in gas permeability and selectivity were calculated as follows:

$$\%\ \text{change in } P_i = \left(\frac{P_i^{\text{MOF/COF/polymer MMM}} - P_i^{\text{COF/polymer MMM}}}{P_i^{\text{COF/polymer MMM}}} \right) \times 100 \quad (8)$$

$$\%\ \text{change in } S_{i/j} = \left(\frac{S_{i/j}^{\text{MOF/COF/polymer MMM}} - S_{i/j}^{\text{COF/polymer MMM}}}{S_{i/j}^{\text{COF/polymer MMM}}} \right) \times 100 \quad (9)$$

Overall, we calculated the gas permeabilities and selectivities of 576,219 MOF/COF/polymer MMMs for CO_2/N_2, 1193 MOF/COF/polymer MMMs for CO_2/CH_4, 200,424 MOF/COF/polymer MMMs for H_2/CH_4, 156,283 MOF/COF/polymer MMMs for H_2/N_2, and 32,211 MOF/COF/polymer MMMs for H_2/CO_2 separations.

3. RESULTS AND DISCUSSION

After computing the permeability and selectivity of dual filler-incorporated MMMs, we examined their locations with respect to the upper bound for each gas separation as we will discuss in detail below. Many MOF/COF/polymer MMMs were found to exceed the upper bound. The number of MOF/COF/polymer MMMs that can exceed the upper bound for each gas separation of interest is given in Table 1 together with the corresponding number of COF/polymer MMMs and MOF/polymer MMMs used for their modeling. As an example for reading the table, 120 COF/PTMSP-co(95/5) MMMs were found to be below the upper bound for H_2/N_2 separation. These 120 COF/PTMSP-co(95/5) MMMs and 1193 MOF/PTMSP-co(95/5) MMMs were combined to generate 143,160 MOF/COF/PTMSP-co(95/5) MMMs. 41,603 MMMs exceeded the upper bound, and they were generated from combinations of 115 COF/PTMSP-co(95/5) MMMs and 652 MOF/PTMSP-co(95/5) MMMs.

3.1. CO_2/N_2 Separation. We calculated CO_2 permeabilities and CO_2/N_2 selectivities of 480 COF/PTMSP MMMs, which were all located below the upper bound (red data), and 1193 MOF/PTMSP MMMs (blue data) as shown in Figure 1a. MOF/COF/PTMSP MMMs (572,640) were generated from them, and their CO_2 permeabilities and CO_2/N_2 selectivities were computed. A total of 119,622 MMMs out of 572,640 MOF/COF/polymer MMMs exceeded the Robeson's upper bound as shown in Figure 1b. Throughout this work, we specifically focused on the MOF/COF/polymer MMMs that exceed the upper bound and compared their gas permeability and selectivity with those of COF/polymer

https://doi.org/10.1021/acs.iecr.2c04500
Ind. Eng. Chem. Res. 2023, 62, 2924−2936

Table 1. The Numbers of MOF/COF/Polymer MMMs That Exceed the Upper Bound and the Numbers of MOF/Polymer and COF/Polymer MMMs Used to Generate Them

polymer	MOF/COF/polymer MMM	COF/polymer MMM	MOF/polymer MMM
	CO_2/N_2		
PTMSP	119,622	375	652
PIM-1	2020	2	1104
	CO_2/CH_4		
PIM-1	1143	1	1143
	H_2/CH_4		
PTMSP-co(95/5)	40,904	158	574
Teflon AF-2400	7830	8	1143
	H_2/N_2		
PTMSP-co(95/5)	41,603	115	653
PIM-1	9735	9	1131
	H_2/CO_2		
PTMSP-co(95/5)	22,090	27	1018

MMMs that were below the upper bound to understand how incorporation of a second type of filler, a MOF, can improve the gas separation performance of a COF-incorporated polymer membrane.

CO_2 permeabilities and CO_2/N_2 selectivities of MOF/COF/polymer MMMs that exceed the upper bound are shown in Figure 2 together with permeabilities and selectivities of MOF/polymer MMMs and COF/polymer MMMs that were used to generate them. We considered two different polymers, PTMSP and PIM-1, as the matrix of MMMs for CO_2/N_2 separation. PTMSP has a very high CO_2 permeability and mediocre CO_2/N_2 selectivity (29,000 Barrer and 10.7, respectively), whereas PIM-1 has a relatively high CO_2/N_2 selectivity (25) with a CO_2 permeability of 2300 Barrer. We examined how gas separation performances of these two polymers are changed by the addition of dual fillers, MOFs and COFs.

Figure 2a shows CO_2 permeabilities and CO_2/N_2 selectivities of 119,622 MOF/COF/PTMSP MMMs (green data) generated from the combinations of 375 COF/PTMSP MMMs (red data) and 652 MOF/PTMSP MMMs (blue data). CO_2 permeabilities of MOF/PTMSP MMMs were computed to be generally higher, 4.14×10^4–4.95×10^4 Barrer, than those of COF/PTMSP MMMs, 3.86×10^4–4.50×10^4 Barrer. Similarly, CO_2/N_2 selectivities of MOF/PTMSP MMMs were calculated to be higher (9.6–10.9) than those of COF/PTMSP MMMs (8.9–9.8). Thus, the resulting MOF/COF/PTMSP MMMs have a higher CO_2 permeability, 4.10×10^4–4.72×10^4 Barrer, and a higher CO_2/N_2 selectivity, 9.6–10.3, compared to COF/PTMSP MMMs. Figure 2b shows that out of 3579 MOF/COF/PIM-1 MMMs, 2020 MOF/COF/PIM-1 MMMs (green data) generated from 2 COF/PIM-1 MMMs (red data) and 1104 MOF/PIM-1 MMMs (blue data) exceed the upper bound. CO_2 permeabilities and CO_2/N_2 selectivities of these 2020 MOF/COF/polymer MMMs were computed to vary between 3.68×10^3 and 3.82×10^3 Barrer and 23.2 and 24.1, respectively, while CO_2 permeabilities and CO_2/N_2 selectivities of COF/PIM-1 MMMs are in between 3.53×10^3 and 3.63×10^3 Barrer and 22.0 and 23.3, respectively.

These results show the high potential of improving gas separation performance of only COF-incorporated MMMs by the addition of the MOFs as the second filler type. To better understand the results, we focused on MOF/COF/PTMSP MMMs, which overcome the upper bound by showing (i) an increase both in CO_2 permeability and CO_2/N_2 selectivity, (ii) an increase both in CO_2 and N_2 permeabilities without any change in CO_2/N_2 selectivity, and (iii) an increase in CO_2/N_2 selectivity especially due to the decrease in N_2 permeability compared to separation performances of COF/PTMSP MMMs. To quantify how incorporation of a second type of filler, a MOF, can improve the gas separation performance of a COF-incorporated polymer membrane, we calculated the percent changes in CO_2 permeabilities, N_2 permeabilities, and CO_2/N_2 selectivities of 119,622 MOF/COF/PTMSP MMMs with respect to 375 COF/PTMSP MMMs. Figure S2 shows that when MOF and COF fillers are used together in PTMSP instead of only a COF filler, percent changes in P_{CO_2}, P_{N_2}, and S_{CO_2/N_2} varied between −4 and 13%, −9 and 7%, and −1 and 11%, respectively. We presented these percent changes for a representative set of MOF/COF/PTMSP MMMs in Figure 3a–c where x and y axes illustrate the identity of COFs and MOFs in COF/PTMSP MMMs and MOF/PTMSP MMMs used for generating MOF/COF/PTMSP MMMs. If there is a more than 2% increase in the permeability or selectivity of an MOF/COF/PTMSP MMM compared to that of a corresponding COF/PTMSP MMM, the MOF–COF

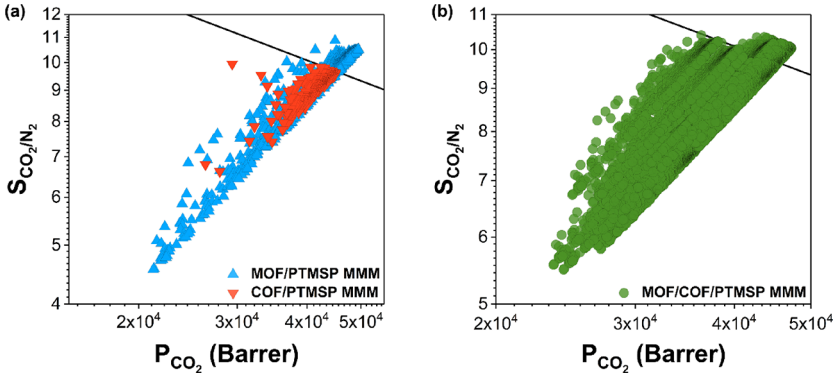


Figure 1. Calculated CO_2 permeabilities and CO_2/N_2 selectivities of (a) 480 COF/PTMSP MMMs and 1193 MOF/PTMSP MMMs and (b) 572,640 MOF/COF/PTMSP MMMs generated from them. Robeson's upper bound is shown with the black line.

https://doi.org/10.1021/acs.iecr.2c04500
Ind. Eng. Chem. Res. 2023, 62, 2924–2936

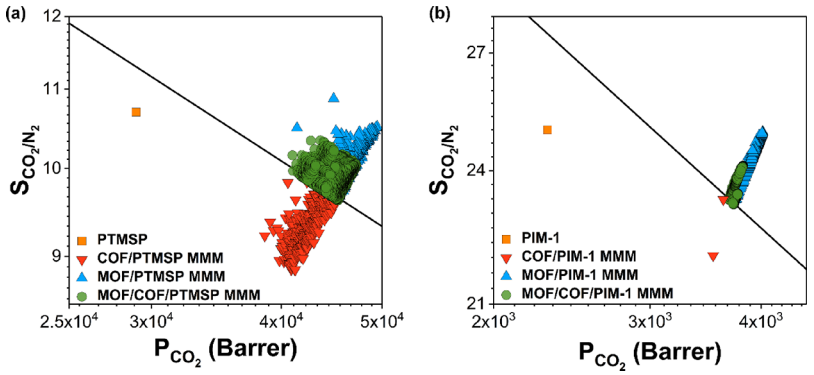


Figure 2. Calculated CO_2 permeabilities and CO_2/N_2 selectivities of (a) 652 MOF/PTMSP MMMs, 375 COF/PTMSP MMMs, and 119,622 MOF/COF/PTMSP MMMs generated from them and (b) 1104 MOF/PIM-1 MMMs, 2 COF/PIM-1 MMMs, and 2020 MOF/COF/PIM-1 MMMs generated from them. Robeson's upper bound is shown with the black line.

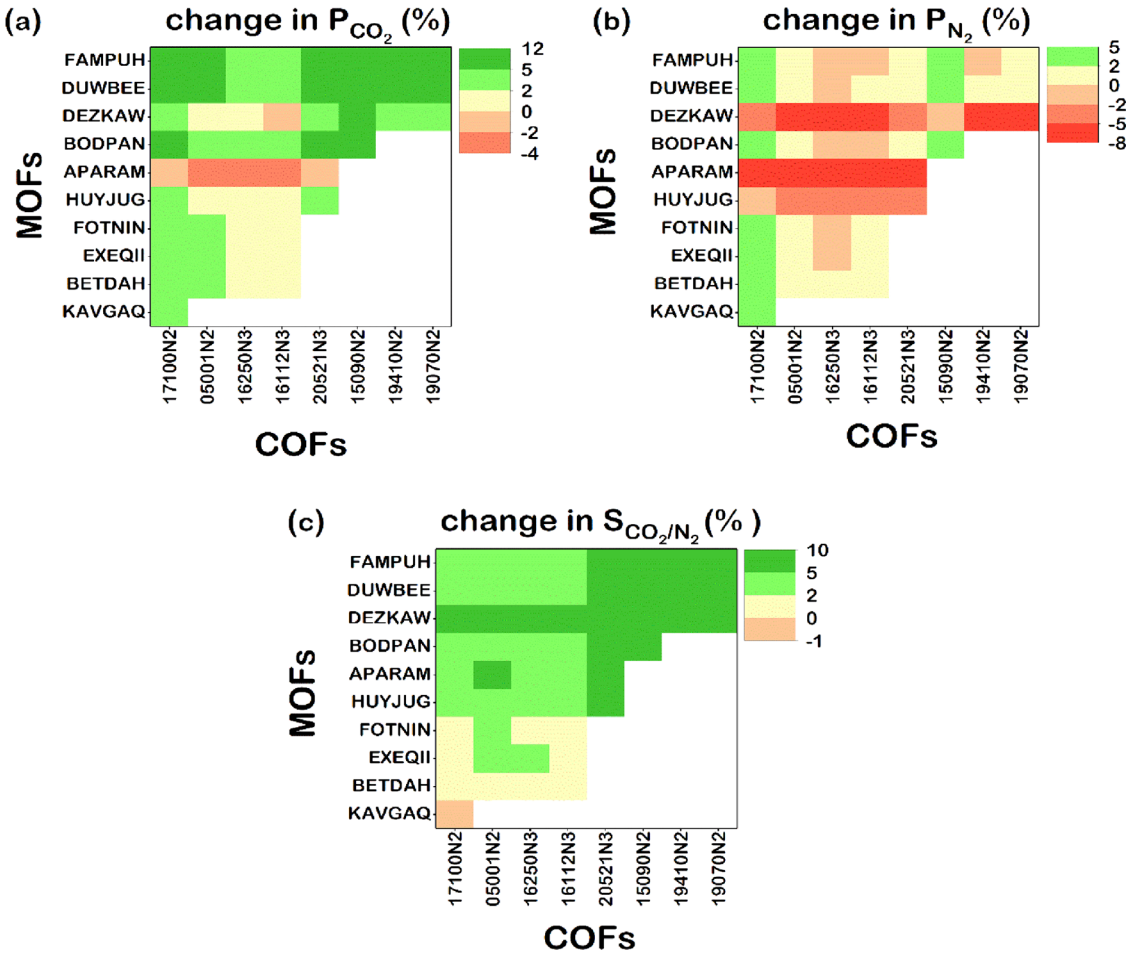


Figure 3. Calculated percent changes in (a) CO_2 permeabilities, (b) N_2 permeabilities, and (c) CO_2/N_2 selectivities of representative MOF/COF/PTMSP MMMs with respect to COF/PTMSP MMMs for the selected set of MOF−COF pairs.

matching is shown with green. If using dual fillers instead of using only a COF filler in MMMs causes a small change of 0−2% (a decrease) in the permeability or selectivity, the MOF−COF matching is shown with yellow (red). If the resulting MOF/COF/polymer MMM still remains below the upper bound, it is shown by white. For example, when the MOF, DUWBEE, and the COF, 15090N2, were used together in PTMSP, the resulting MMM surpasses the upper bound thanks to an 11.7% (5.3%) increase in CO_2 (N_2) permeability and a 6.1% increase in selectivity compared to the only COF-incorporated polymer membrane, the 15090N2/PTMSP MMM. Here, the MOF, DUWBEE, offers a very high CO_2 permeability (1.28×10^6 Barrer), which can be attributed to its high CO_2 uptake (2.19 mol/kg) and fast CO_2 diffusion (2.02×10^{-4} cm^2/s). On the other hand, the COF, 15090N2, is much less CO_2-permeable (1.27×10^5 Barrer) due to its lower CO_2 adsorption (0.98 mol/kg) and slower diffusivity (7.99×10^{-5} cm^2/s). A MOF/COF/polymer MMM example with improved selectivity is the HUYJUG/20521N3/PTMSP MMM where incorporation of HUYJUG and 20521N3 into PTMSP

https://doi.org/10.1021/acs.iecr.2c04500
Ind. Eng. Chem. Res. 2023, 62, 2924−2936

resulted in a membrane with a 2.9% higher CO_2 permeability, a 2.8% lower N_2 permeability, and a 5.8% higher selectivity compared to the only COF-incorporated membrane. The HUYJUG/20521N3/PTMSP MMM overcomes the upper bound by a CO_2 permeability of 4.39×10^4 Barrer and a CO_2/N_2 selectivity of 9.9. Another interesting example is the FOTNIN/17100N2/PTMSP MMM, which overcomes the upper bound due to a ~4% increase in CO_2 and N_2 permeabilities without a significant change in CO_2/N_2 selectivity. The increase in gas permeabilities is attributed to higher CO_2 and N_2 permeabilities of the FOTNIN/PTMSP MMM (4.64×10^4 and 4.68×10^3 Barrer, respectively) compared to those of the 17100N2/PTMSP MMM (4.30×10^4 and 4.38×10^3 Barrer, respectively).

For MOF/COF/PIM-1 MMMs, the percent changes in CO_2 permeability, N_2 permeability, and CO_2/N_2 selectivity are shown in Figure S3. The maximum increase in CO_2 permeability was calculated as 6.63% when dual fillers (a MOF and a COF) were used instead of using only a COF filler in PIM-1. For all MOF/COF/PIM-1 MMMs, however, the percent change in N_2 permeabilities was found to be relatively low (between −0.2 and 1.7%). Therefore, most of the MOF/COF/PIM-1 MMMs have a higher CO_2/N_2 selectivity compared to COF/polymer MMMs. Overall, our results showed that when a polymer with a relatively high gas permeability ($\geq 10^4$ Barrer) like PTMSP is selected, CO_2/N_2 selectivities of the MOF/COF/polymer MMMs can be almost the same with or higher than the CO_2/N_2 selectivities of the COF/polymer MMMs. On the other hand, for a polymer with a mediocre gas permeability (~10^3 Barrer) like PIM-1, the number of COF/PIM-1 MMMs located below the upper bound is lower than the number of COF/PTMSP and COF/PTMSP-co(95/5) MMMs, and using a MOF as the second filler to generate MOF/COF/PIM-1 MMMs slightly improves their CO_2 permeability and CO_2/N_2 selectivity.

3.2. CO_2/CH_4 Separation. Almost all COF/PIM-1 MMMs among 589 COF/PIM-1 MMMs overcome the upper bound for CO_2/CH_4 separation except one (21040N3/PIM-1) as shown in Figure 4. When the COF filler, 21040N3, was used together with a MOF filler in PIM-1, 1143 out of 1193 MOF/21040N3/PIM-1 MMMs surpassed the upper bound. Figure 4 shows calculated CO_2 permeabilities and CO_2/CH_4 selectivities of 1143 MOF/COF/PIM-1 MMMs (green data) generated from the combinations of 21040N3/PIM-1 MMM (red data) and 1143 MOF/PIM-1 MMMs (blue data). All the MOF/PIM-1 MMMs have a higher CO_2 permeability (in the range of 3.51×10^3–4.02×10^3 Barrer) than the 21040N3/PIM-1 MMM (3.39×10^3 Barrer). Similarly, CO_2/CH_4 selectivities of MOF/PIM-1 MMMs were calculated to be higher (16.2–18.4) than that of the 21040N3/PIM-1 MMM (15.7). Thus, the resulting MOF/COF/PIM-1 MMMs have a higher CO_2 permeability, in the range of 3.45×10^3–3.69×10^3 Barrer, and a slightly higher CO_2/CH_4 selectivity, up to 17, compared to the 21040N3/PIM-1 MMM. The addition of MOF fillers to the 21040N3/PIM-1 MMM led to a percent increase in CO_2 permeabilities between 1.8 and 8.9% and a percent increase in CO_2/CH_4 selectivities between 1.7 and 8.2% as shown in Figure S4. For example, when the 21040N3/PIM-1 MMM was combined with the CUFFEP/PIM-1 MMM, the MOF, CUFFEP, provided about an 8.8% increase in CO_2 permeability. 21040N3 has low CO_2 and CH_4 permeabilities (1.71×10^4 and 1.58×10^4 Barrer, respectively), which can be attributed to slow diffusion of CO_2 and CH_4 (1.63×10^{-6} and 4.05×10^{-6} cm^2/s, respectively) in the COF. On the other hand, fast CO_2 diffusion (1.87×10^{-4} cm^2/s) in the MOF led to a high CO_2 permeability (1.57×10^6 Barrer). As a result, the CUFFEP/21040N3/PIM-1 MMM overcomes the upper bound with a CO_2 permeability of 3.69×10^3 Barrer and a CO_2/CH_4 selectivity of 17.

As another example, the MOF FECKAA leads to the smallest percentage increase in CO_2 permeability (1.8%) since the CO_2 permeability of the FECKAA/PIM-1 MMM (3.51×10^3 Barrer) is close to that of the 21040N3/PIM-1 MMM (3.39×10^3 barrer). Still, even this slight increase in CO_2 permeability with the use of FECKAA together with 21040N3 in PIM-1 is enough to locate the FECKAA/21040N3/PIM-1 MMM over the upper bound with a CO_2 permeability of 3.45 $\times 10^3$ Barrer and a CO_2/CH_4 selectivity of 16. Overall, these results indicate that any COF can be incorporated into PIM-1 to obtain MMMs above the upper bound for CO_2/CH_4 separation if one of the 1143 MOFs is also used as the second filler in PIM-1.

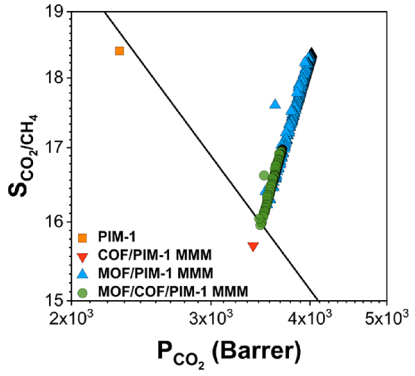


Figure 4. Calculated CO_2 permeabilities and CO_2/CH_4 selectivities of 1143 MOF/PIM-1 MMMs, 21040N3/PIM-1 MMM, and 1143 MOF/COF/PIM-1 MMMs generated from them. Robeson's upper bound is shown with the black line.

3.3. H_2/CH_4, H_2/N_2, and H_2/CO_2 Separations. For H_2/CH_4 separation, we examined two different polymers, PTMSP-co(95/5) and Teflon AF-2400. PTMSP-co(95/5) is a highly permeable polymer with a relatively low selectivity (P_{H_2}: 20,400 Barrer, S_{H_2/CH_4}: 0.953). We calculated H_2 permeabilities and H_2/CH_4 selectivities of 189,687 MOF/COF/PTMSP-co(95/5) MMMs generated from 159 COF/PTMSP-co(95/5) MMMs and 1193 MOF/PTMSP-co(95/5) MMMs. MOF/PTMSP-co(95/5) MMMs have higher H_2 permeabilities and much higher H_2/CH_4 selectivities (P_{H_2}: 2.42×10^4–3.50×10^4 Barrer, S_{H_2/CH_4}: 0.9–1.8) than those of COF/PTMSP-co(95/5) MMMs (P_{H_2}: 1.67×10^4–3.11×10^4 Barrer, S_{H_2/CH_4}: 0.7–1.0), which were used to generate MOF/COF/PTMSP-co(95/5) MMMs above the upper bound. As a result, as shown in Figure 5a, 40,904 MOF/COF/PTMSP-co(95/5) MMMs (green data) generated from 158 COF/PTMSP-co(95/5) MMMs (red data) and 574 MOF/PTMSP-co(95/5) MMMs (blue data) overcome the upper bound with H_2 permeabilities and H_2/CH_4 selectivities in the ranges of 2.24×10^4–3.29×10^4 Barrer and 0.9–1.3, respectively. Changes in H_2 and CH_4 permeability and H_2/CH_4 selectivity of MMMs are presented in Figure S5. Many MOF/COF/PTMSP-co(95/

https://doi.org/10.1021/acs.iecr.2c04500
Ind. Eng. Chem. Res. 2023, 62, 2924–2936

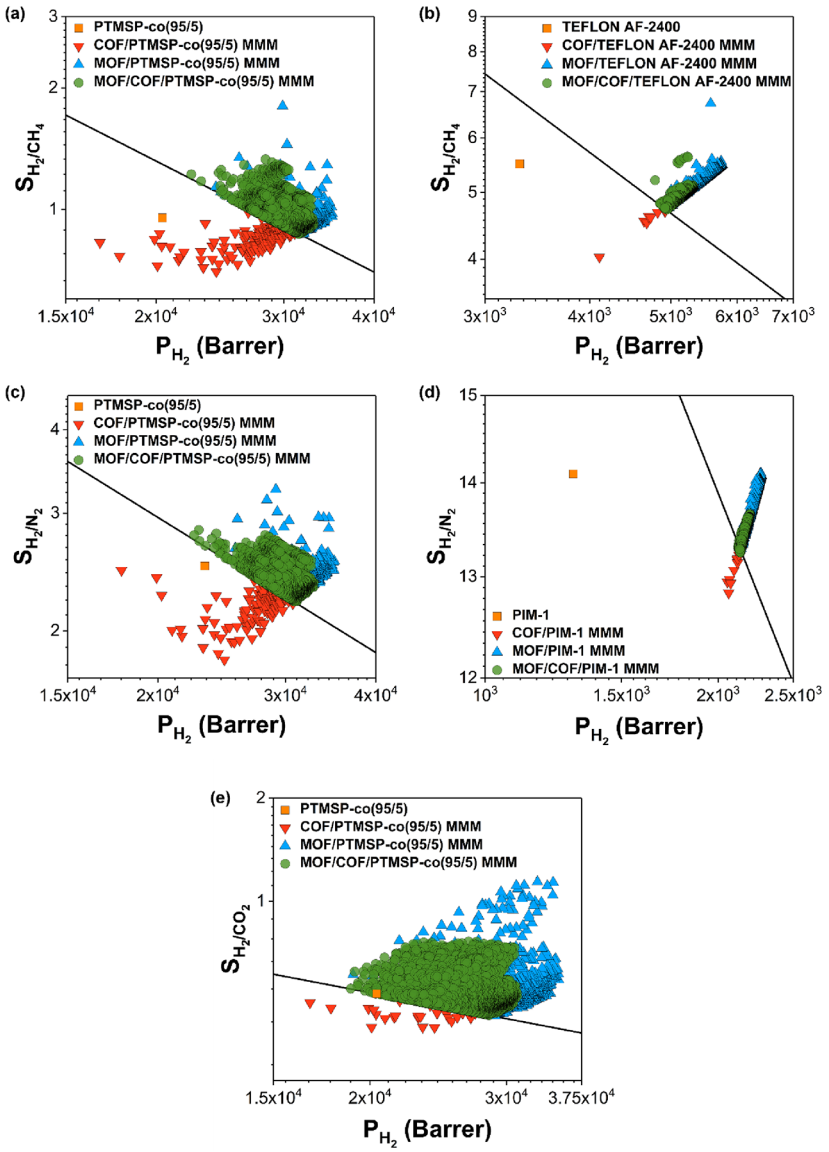


Figure 5. Calculated H_2 permeability and H_2/CH_4 selectivity of (a) 574 MOF/PTMSP-co(95/5), 158 COF/PTMSP-co(95/5), and 40,904 MOF/COF/PTMSP-co(95/5) MMMs and (b) 1143 MOF/Teflon AF-2400, 8 COF/Teflon AF-2400, and 7830 MOF/COF/Teflon AF-2400 MMMs. Calculated H_2 permeability and H_2/N_2 selectivity of (c) 653 MOF/PTMSP-co(95/5), 115 COF/PTMSP-co(95/5), and 41,603 MOF/COF/PTMSP-co(95/5) MMMs and (d) 1131 MOF/PIM-1, 9 COF/PIM-1, and 9735 MOF/COF/PIM-1 MMMs. Calculated H_2 permeability and H_2/CO_2 selectivity of (e) 1018 MOF/PTMSP-co(95/5), 27 COF/PTMSP-co(95/5), and 22,090 MOF/COF/PTMSP-co(95/5) MMMs. Robeson's upper bound is shown with the black line.

5) MMMs exceed the upper bound thanks to the change in their P_{H_2} (up to 34%).

We then focused on Teflon AF-2400 to investigate the effects of using dual fillers in a relatively more H_2-selective polymer (P_{H_2}: 3300 Barrer, S_{H_2/CH_4}: 5.5). We calculated H_2 permeabilities and H_2/CH_4 selectivities of 10,737 MOF/COF/Teflon AF-2400 MMMs generated from 9 COF/Teflon AF-2400 MMMs and 1193 MOF/Teflon AF-2400 MMMs. MOF/COF/Teflon AF-2400 MMMs (7830) (green data) generated from 8 COF/Teflon AF-2400 MMMs (red data) and 1143 MOF/Teflon AF-2400 MMMs (blue data) surpassed the Robeson's upper bound as shown in Figure 5b. H_2 permeabilities and H_2/CH_4 selectivities of MOF/Teflon AF-2400 MMMs (4.93×10^3–5.76×10^3 Barrer and 4.8–6.7, respectively) were found to be much higher than those of COF/Teflon AF-2400 MMMs (4.11×10^3–4.92×10^3 Barrer and 4.0–4.7, respectively).

As a result, incorporation of a MOF filler into Teflon AF-2400 together with a COF filler led to an increase in H_2 permeability up to 16.5% and in H_2/CH_4 selectivity up to 29.3% as shown in Figure S6 compared to H_2 permeability and H_2/CH_4 selectivity of COF/Teflon AF-2400 MMMs. H_2 permeabilities of MOF/COF/Teflon AF-2400 MMMs exceeding the upper bound were found to be in the range of 4.79×10^3–5.32×10^3 Barrer, and their H_2/CH_4 selectivities varied between 4.7 and 5.6. These results suggest that, for dual filler-incorporated PTMSP-co(95/5) MMMs, the MOF–COF pair choice should be carefully made since the MOF can increase or decrease H_2 and CH_4 permeabilities of COF/PTMSP-co(95/5) MMMs. It is more straightforward to use different MOFs and COFs as fillers if the polymer matrix is Teflon AF-2400

https://doi.org/10.1021/acs.iecr.2c04500
Ind. Eng. Chem. Res. 2023, 62, 2924–2936

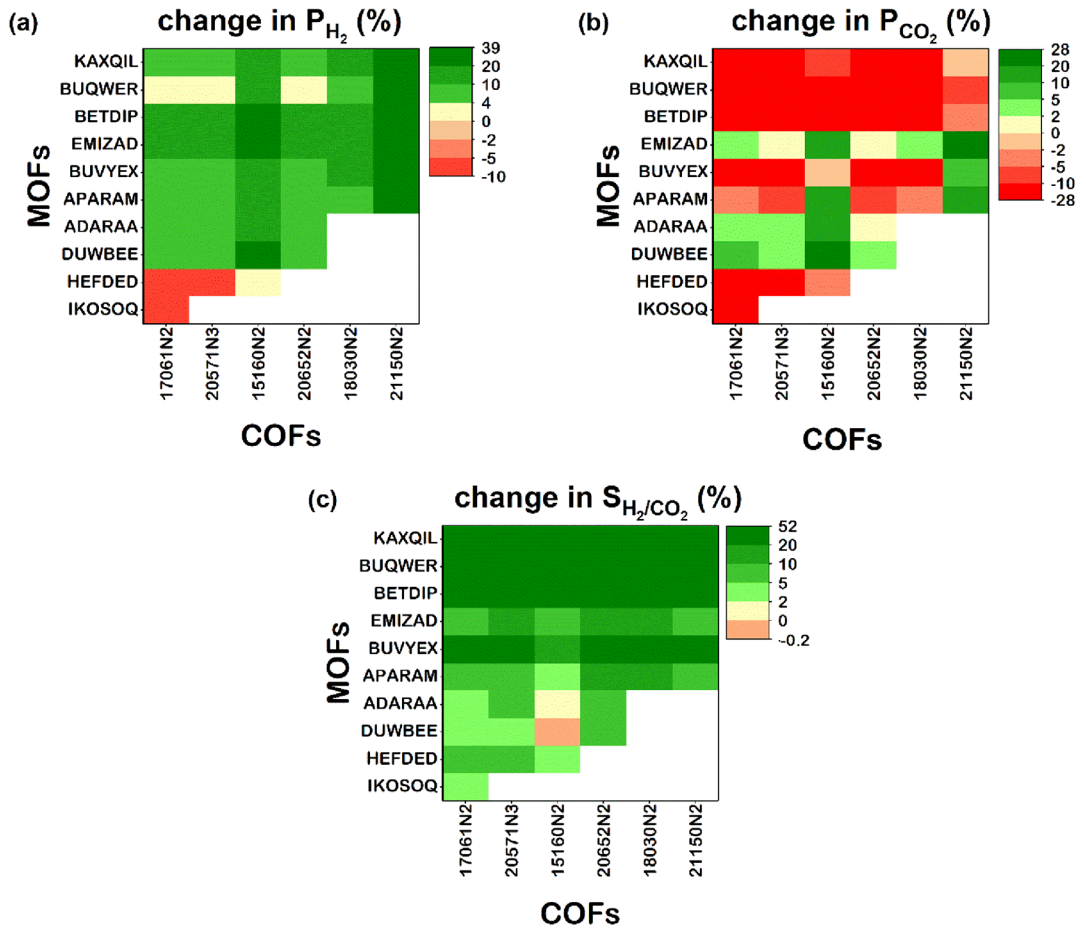


Figure 6. Calculated percent changes in (a) H_2 permeabilities, (b) CO_2 permeabilities, and (c) H_2/CO_2 selectivities of representative MOF/COF/PTMSP-co(95/5) MMMs with respect to COF/PTMSP-co(95/5) MMMs.

since addition of the MOF into COF/Teflon AF-2400 MMMs generally improves the H_2 permeability and H_2/CH_4 selectivities while does not significantly change CH_4 permeabilities.

For H_2/N_2 separation, we focused on two polymers, PTMSP-co(95/5) and PIM-1, and calculated H_2 permeabilities and H_2/N_2 selectivities of MOF/COF/PTMSP-co(95/5) and MOF/COF/PIM-1 MMMs. A total of 143,160 MOF/COF/PTMSP-co(95/5) MMMs were studied for H_2/N_2 separation. MOF/PTMSP-co(95/5) MMMs (653) (blue data) and 115 COF/PTMSP-co(95/5) MMMs (red data) have H_2 permeabilities in the range of 2.56×10^4−3.5×10^4 and 1.78×10^4−3.07×10^4 Barrer, respectively. These wide ranges of H_2 permeabilities led to 41,603 types of MOF/COF/PTMSP-co(95/5) MMMs (green data in Figure 5c) surpassing the upper bound with high H_2 permeabilities (2.24×10^4−3.28×10^4 Barrer). Figure S7 demonstrates that H_2 permeabilities and H_2/N_2 selectivities of dual filler-incorporated MMMs were improved up to 39.1 and 32.6% compared to those of COF/PTMSP-co(95/5) MMMs, respectively, which means that the MOF filler plays a significant role in determining the H_2 permeability and H_2/N_2 selectivity of the MOF/COF/PTMSP-co(95/5) MMMs.

PIM-1 has a moderate H_2/N_2 selectivity (14.1) and H_2 permeability (1300 barrer). When PIM-1 is used as the matrix of MMMs, 9735 MOF/COF/PIM-1 MMMs (green data in Figure 5d) generated from 9 COF/PIM-1 MMMs (red data) and 1131 MOF/PIM-1 MMMs (blue data) overcome Robeson's upper bound among a total of 13,123 MOF/COF/PIM-1 MMMs. H_2 permeabilities of 1131 MOF/PIM-1 MMMs and 9 COF/PIM-1 MMMs vary between 2.14×10^3 and 2.27×10^3 and 2.05×10^3 and 2.13×10^3 Barrer, respectively, and their H_2/N_2 selectivities were found to vary between 13.3−14.1, and 12.8−13.2, respectively, as shown in Figure 5d. As a result, 9735 MOF/COF/PIM-1 MMMs above the upper bound have H_2 permeability and H_2/N_2 selectivity in the range of 2.12×10^3−2.20×10^3 Barrer and 13.3−13.7, respectively. As Figure S8 shows, addition of the MOF filler increased the H_2 permeability and H_2/N_2 selectivity of MOF/COF/PIM-1 MMMs up to 5.2 and 4.8%.

Finally, for H_2/CO_2 separation, H_2 permeabilities and H_2/CO_2 selectivities were calculated for a total of 32,211 MOF/COF/PTMSP-co(95/5) MMMs generated from 27 COF/PTMSP-co(95/5) MMMs below the upper bound and 1193 MOF/PTMSP-co(95/5) MMMs. One thousand eighteen of 1193 MOF fillers improved the H_2/CO_2 separation performances of all 27 COF-incorporated PTMSP-co(95/5) membranes. MOF/COF/PTMSP-co(95/5) MMMs (22,090) surpassed the upper bound for H_2/CO_2 separation with H_2 permeabilities of 1.89×10^4−3.09×10^4 Barrer as shown with green data in Figure 5e. The percent increases in H_2 permeabilities of dual filler-incorporated PTMSP-co(95/5) membranes compared to those of only COF-incorporated MMMs reached up to 45% as shown in Figure S9. Similar to H_2/CH_4 separation, it is required to choose a suitable MOF−COF pair to incorporate into PTMSP-co(95/5) since the

https://doi.org/10.1021/acs.iecr.2c04500
Ind. Eng. Chem. Res. 2023, 62, 2924−2936

MOF filler can cause an undesirable decrease in H_2 and CO_2 permeabilities of the MMMs.

The percent changes in H_2 permeability, CO_2 permeability, and H_2/CO_2 selectivity for a representative set of MOF/COF/PTMSP-co(95/5) MMMs are shown in Figure 6. For example, when the MOF, KAXQIL, and the COF, 15160N2, were used together in PTMSP-co(95/5), both H_2 permeability and H_2/CO_2 selectivity of the MMM increased by 17 and 27%, respectively, compared to those of only COF-incorporated MMMs. A higher self-diffusivity of H_2 in the MOF, KAXQIL (1.08×10^{-3} cm^2/s), compared to that in the COF, 15160N2 (5.30×10^{-4} cm^2/s), led to a much higher H_2 permeability of the MOF (1.46×10^5 Barrer) compared to the COF (2.84×10^4 Barrer). Another promising MOF−COF pair is ADARAA and 15160N2, which led to a 20% higher H_2 and CO_2 permeability compared to using only 15160N2 in PTMSP-co(95/5). As a result, the ADARAA/15160N2/PTMSP-co(95/5) MMM overcomes the upper bound. Overall, these results show the great promise of using two types of dual fillers in polymer membranes for H_2 separation.

To understand how the identity of MOF fillers affects the gas separation performances of dual filler-incorporated polymer membranes, we specifically focused on two MOF−COF pairs, KAXQIL-17061N2 and IKOSOQ-17061N2 with the same COF, 17061N2. The KAXQIL/PTMSP-co(95/5) MMM has a slightly higher H_2 permeability (2.99×10^4 Barrer) than the 17061N2/PTMSP-co(95/5) MMM (2.70×10^4 Barrer). This was attributed to the high H_2 permeability of KAXQIL (1.46×10^5 Barrer) due to high H_2 diffusivity (1.08×10^{-3} cm^2/s) in this MOF. On the other hand, the IKOSOQ/PTMSP-co(95/5) MMM exhibited a lower H_2 permeability (2.24×10^4 Barrer) than the 17061N2/PTMSP-co(95/5) MMM since the COF filler is more H_2-permeable (7.86×10^4 Barrer) than the MOF, IKOSOQ (3.19×10^4 Barrer). Therefore, depending on the MOF−COF pair, an MOF/COF/polymer can exceed the upper bound as a result of an increase in permeability and selectivity together or due to an increase in selectivity only.

To explain why MOF/COF/polymer MMMs exhibit higher gas permeabilities with respect to those of only COF-incorporated MMMs, we examined the structural and chemical properties of MOFs and COFs. Gas permeability is a result of complex interplay of several physical and chemical properties, and it is difficult to isolate the impact of each property on the gas permeability. We aimed to focus on structural properties mainly driving the materials' affinity toward a gas species and focused on the top MOFs, which led to the highest percent increase in CO_2 permeabilities of MOF/COF/PTMSP MMMs compared to COF/PTMSP MMMs for CO_2/N_2 separation. Table S4 presents the structural properties of the top 15 MOF fillers that led to the highest increase in CO_2 permeabilities when utilized in MOF/COF/PTMSP MMMs. These top 15 MOF fillers were found to have some common structural properties such as moderate PLDs (between 4.28 and 11.7 Å), high porosities (0.66−0.75), relatively high LCDs (5.87−12.16 Å), and large S_{acc} (2229.2−4307.1 m^2/g). These relatively high porosities and LCD values lead to high CO_2 permeabilities of MOFs. On the other hand, the COF used in these dual filler-incorporated polymer membranes has larger PLD and LCD values (9.49 and 9.92 Å, respectively), a smaller accessible surface area (607.2 m^2/g), and a smaller porosity (0.48) compared to the top 15 MOF fillers. We also examined the organic units of each framework; except an MOF, CORZIU, all the top 15 MOFs have benzene-based ligands, and 5 of the top MOFs have amine-based ligands in agreement with the previous reports showing that amine-based ligands in frameworks provide high CO_2 affinities,[40,41] which generally lead to high CO_2 permeability. The most common metals in MOFs that we studied are zinc (Zn), found in 260 MOFs, copper (Cu) in 230 MOFs, cadmium (Cd) in 127 MOFs, and cobalt (Co) in 126 MOFs, as shown in Figure S10. Four of the top MOFs have Zn and Cd metals, and 3 of them include nickel (Ni). High CO_2 uptakes of 11 MOFs, which have Zn and Cd, can be attributed to the stronger interaction between CO_2 molecules and these metals (energetic interaction values, ε/k_B, for these metals are 62.4 and 114.8 K, respectively). Although Ni has a relatively low ε/k_B value (7.6 K), three MOFs with Ni have a very large surface areas (>3600 m^2/g), and they also include amine-based ligands and fluorine. All these factors resulted in high CO_2 uptakes and hence high CO_2 permeabilities for these MOFs.

Table S5 shows PLD, LCD, S_{acc}, and porosity of the top 15 MOF fillers, which led to the highest increase in H_2 permeabilities of MOF/COF/PTMSP-co(95/5) MMMs, and the COF fillers used to generate these MMMs for H_2/CH_4, H_2/N_2, and H_2/CO_2 separations. PLD, LCD, and porosities of the top MOFs are generally larger (9.24−34.51 Å, 18.21−37.53 Å, and 0.64−0.93, respectively) than those of COFs used to generate the dual filler-incorporated membranes (4.86−13.23 Å, 6.31−13.64 Å, and 0.62−0.63, respectively). Smaller PLDs, LCDs, and porosities of COFs lead to low H_2 permeabilities. When these MOFs and COFs were incorporated into PTMSP-co(95/5), the generated MOF/COF/PTMSP-co(95/5) MMMs show higher H_2 permeabilities compared to COF/PTMSP-co(95/5) MMMs. Thirteen out of the 15 MOFs have amine-based ligands. Among the top 15 MOFs, Cu was found in 5 MOFs, and Zn was found in 3 MOFs. Among these top 15 MOFs, there are MOFs with Zn and indium (In) (ε/k_B values for LJ interactions are 62.4 and 301.6 K, respectively), which lead to relatively high H_2 uptakes and large porosities that lead to H_2 diffusivities, providing high H_2 permeabilities. On the other hand, COFs listed in Table S5 offer lower H_2 uptakes and diffusivities and hence lower H_2 permeabilities than the top MOFs.

In this work, we computed gas separation performances of almost a million types of MOF/COF/polymer MMMs, and our computations have several assumptions that need to be discussed. These assumptions may not be valid in real applications, but they save enormous computational time when a million of MMMs has been studied. We assumed rigid MOFs and COFs in molecular simulations and modeled MMMs as defect-free structures. The Maxwell permeation model, which assumes an ideal morphology without considering voids, filler agglomeration, and polymer rigidification in the MMM, was used to predict the gas permeabilities of MMMs. It should be noted that fillers in MMMs can cause an increased rigidity at the polymer−filler interface, which indicates a good compatibility and adhesion at the organic−inorganic interfaces between fillers and polymers.[42] The morphologies of fillers and filler agglomeration, which depends on many intrinsic factors such as the degree of dispersion of particles and the surface area of particles, can affect the gas separation performances of MMMs.[43,44] Our simulations do not provide any information about these issues.

There are also recent examples of core-and-shell MOF@COF (a MOF confined in the pore of a COF) composites

https://doi.org/10.1021/acs.iecr.2c04500
Ind. Eng. Chem. Res. 2023, 62, 2924−2936

incorporated into a polymer for gas separation applications. A UiO-66-NH_2@TpPa-1 composite was recently incorporated into polysulfone (PSF) to be utilized as a filler in an MMM for the separation of an equimolar CO_2/CH_4 mixture at 1 bar and 298 K.[21] Due to the high compatibility of the COF in the outer layer with the polymer matrix, nonselective void formation between the filler and the polymer was avoided, which led to an increase in CO_2/CH_4 selectivity and CO_2 permeability. Since our work focused on dual filler-incorporated MOF/COF/polymer membranes instead of MMMs including MOF@COF composites, we did not compare the performances of MOF/COF/polymer MMMs studied in this work with the performances of MOF@COF incorporated polymer MMMs that recently appeared in the literature.

4. CONCLUSIONS

In this work, by combining molecular simulations with theoretical permeation models, we predicted CO_2 capture and H_2 purification performances of the largest number of membranes, 966,330 MOF/COF/polymer MMMs studied to date. All permeability data were obtained at 1 bar and 298 K. Many MOF/COF/polymer MMMs were shown to exceed the upper bounds established for polymers. For H_2 and CO_2 separations, the majority of COF/polymer MMMs below the upper bound overcome the upper bound when an MOF was used as a second type of filler in the MOF/COF/polymer MMM. The CO_2 permeabilities of MOF/COF/PTMSP MMMs and MOF/COF/PIM-1 MMMs were computed to vary between 4.10×10^4 and 4.72×10^4 and 3.68×10^3 and 3.82×10^3 barrer, respectively. These values were significantly higher than the CO_2 permeabilities of neat PTMSP (2.9×10^4 barrer) and PIM-1 (2.3×10^3 barrer) membranes. For CO_2/CH_4 separation, dual filler-incorporated MOF/COF/PIM-1 MMMs were found to have a higher CO_2 permeability, in the range of 3.45×10^3–3.69×10^3 barrer, and a slightly higher CO_2/CH_4 selectivity, up to 17, compared to only COF-incorporated PIM-1 membranes. H_2 permeabilities of MOF/COF/PTMSP-co(95/5) MMMs were calculated to range from 1.89×10^4 to 3.09×10^4 barrer, which are higher than the permeability of a neat polymer membrane, 2.04×10^4 barrer. H_2 permeability (selectivity) of Teflon for H_2/CH_4 and PIM-1 for H_2/N_2 separations were 3.3×10^3 Barrer (5.5) and 1.3×10^3 Barrer (14.1), respectively, whereas those values for MOF/COF/Teflon and MOF/COF/PIM-1 MMMs vary between 4.79×10^3 and 5.32×10^3 Barrer (4.7–5.6) and 2.14×10^3 and 2.20×10^3 Barrer (13.3–13.7). Overall, we examined if there is a significant potential in utilizing dual types of fillers in MMMs to achieve higher gas permeabilities and/or selectivities compared to those offered by the MMMs having a single type of filler. We utilized the enormous data for MOF/polymer MMMs and COF/polymer MMMs that we have produced for the selected polymers having either high gas permeabilities or high gas selectivities. The polymers that we focused on were selected based on the permeability- selectivity limit defined by the Robeson's upper bound introduced in 2008, which is still widely used in high-throughput computational screening studies to compare the gas separation performances of MMMs with that of pure polymers. Therefore, we compared the performances of MOF/COF/polymer MMMs with respect to this upper bound. In future works, the performance of MOF/COF/polymer MMMs should be also investigated for polymers having high permeabilities together with high selectivities, and should be compared with respect to the updated upper bounds.[45,46] It is not trivial to draw an overall conclusion valid for all MOF/COF/polymers since there are cases that using dual fillers in a polymer provides significant improvements in gas separation performance for some MOF/COF/polymer combinations, while for others, it does not make a significant change. However, our results demonstrated that a significant portion of MOF/COF/polymer MMMs surpass the permeability-selectivity limit when dual fillers are used in a polymer instead of merely a COF filler. Therefore, we believe that our results will highlight the potential of MOF/COF/polymer MMMs and accelerate the design and development of novel MOF/COF/polymer MMMs for various gas separations.2 $\times 10^3$ and 2.20 $\times 10^3$ barrer (13.3–13.7). Overall, the aim of this work is to examine if there is a significant potential in utilizing dual types of fillers in MMMs to achieve higher gas permeabilities and/or selectivities compared to those offered by the MMMs having a single type of filler. For this aim, we utilized the enormous data for MOF/polymer MMMs and COF/polymer MMMs that we have produced for the selected polymers having either high gas permeabilities or high gas selectivities. The polymers that we focused on were selected based on the permeability–selectivity limit defined by the Robeson's upper bound introduced in 2008, which is still widely used in high-throughput computational screening studies to compare the gas separation performances of MMMs with that of pure polymers. Therefore, we compared the performances of MOF/COF/polymer MMMs with respect to this upper bound. In future works, the performance of MOF/COF/polymer MMMs should be also investigated with polymers, which have high permeabilities together with high selectivities, and should be compared with respect to the updated upper bounds.[45,46] It is not trivial to draw an overall conclusion valid for all MOF/COF/polymers since there are cases that using dual fillers in a polymer provides significant improvements in gas separation performance for some of the MOF/COF/polymer combinations, while for others, it does not make a significant change. However, our results demonstrated that a significant portion of MOF/COF/polymer MMMs surpass the permeability–selectivity limit when dual fillers are used in a polymer instead of merely a COF filler. Therefore, we believe that our results will highlight the potential of MOF/COF/polymer MMMs and accelerate the design and development of novel MOF/COF/polymer MMMs for various gas separations.

■ ASSOCIATED CONTENT

Supporting Information

The Supporting Information is available free of charge at https://pubs.acs.org/doi/10.1021/acs.iecr.2c04500.

Details for GCMC and MD simulations of COFs and MOFs; experimental gas permeabilities and membrane selectivities of neat polymers for CO_2/N_2, CO_2/CH_4, H_2/CH_4, H_2/N_2, and H_2/CO_2 separations; number of all COF/polymer MMMs, which are below the upper bound and total combinations of MOF/COF/polymer MMMs; comparison of experimental and computed gas permeabilities of MOF/COF/polymer MMMs; percent changes in gas permeabilities and selectivities of MOF/COF/polymer MMMs compared to COF/polymer MMMs for different gas separations; structural properties of the top 15 MOFs as second fillers in MOF/COF/PTMSP MMMs and MOF/COF/PMTSP-co(95/5)

https://doi.org/10.1021/acs.iecr.2c04500
Ind. Eng. Chem. Res. 2023, 62, 2924–2936

MMMs for CO_2 separation and H_2 purification, respectively (PDF)

AUTHOR INFORMATION

Corresponding Author

Seda Keskin − *Department of Chemical and Biological Engineering, Koc University, 34450 Istanbul, Turkey;* orcid.org/0000-0001-5968-0336; Phone: +90(212)338 1362; Email: skeskin@ku.edu.tr

Authors

Sena Aydin − *Department of Computational Science and Engineering, Koc University, 34450 Istanbul, Turkey;* orcid.org/0000-0002-7020-5496

Cigdem Altintas − *Department of Chemical and Biological Engineering, Koc University, 34450 Istanbul, Turkey*

Ilknur Erucar − *Department of Natural and Mathematical Sciences, Ozyegin University, 34794 Istanbul, Turkey;* orcid.org/0000-0002-6059-6067

Complete contact information is available at: https://pubs.acs.org/10.1021/acs.iecr.2c04500

Notes

The authors declare no competing financial interest.

ACKNOWLEDGMENTS

S.K. acknowledges the ERC-2017 starting grant. This research has received funding from the European Research Council (ERC) under the European Union's Horizon 2020 research and innovation program (ERC-2017 starting grant, grant agreement no. 756489-COSMOS).

REFERENCES

(1) Sanders, D. F.; Smith, Z. P.; Guo, R.; Robeson, L. M.; McGrath, J. E.; Paul, D. R.; Freeman, B. D. Energy-efficient polymeric gas separation membranes for a sustainable future: A review. *Polymer* **2013**, *54*, 4729−4761.

(2) Robeson, L. M. The upper bound revisited. *J. Membr. Sci.* **2008**, *320*, 390−400.

(3) Park, H. B.; Kamcev, J.; Robeson, L. M.; Elimelech, M.; Freeman, B. D. Maximizing the right stuff: The trade-off between membrane permeability and selectivity. *Science* **2017**, *356*, No. eaab0530.

(4) Robeson, L. M. Correlation of separation factor versus permeability for polymeric membranes. *J. Membr. Sci.* **1991**, *62*, 165−185.

(5) Hennessy, J. Membranes from academia to industry. *Nat. Mater.* **2017**, *16*, 280−282.

(6) Nunes, S. P.; Culfaz-Emecen, P. Z.; Ramon, G. Z.; Visser, T.; Koops, G. H.; Jin, W.; Ulbricht, M. Thinking the future of membranes: Perspectives for advanced and new membrane materials and manufacturing processes. *J. Membr. Sci.* **2020**, *598*, No. 117761.

(7) Sumer, Z.; Keskin, S. Adsorption- and membrane-based CH_4/N_2 separation performances of MOFs. *Ind. Eng. Chem. Res.* **2017**, *56*, 8713−8722.

(8) Chung, T.-S.; Jiang, L. Y.; Li, Y.; Kulprathipanja, S. Mixed matrix membranes (MMMs) comprising organic polymers with dispersed inorganic fillers for gas separation. *Prog. Polym. Sci.* **2007**, *32*, 483−507.

(9) Liu, G.; Chernikova, V.; Liu, Y.; Zhang, K.; Belmabkhout, Y.; Shekhah, O.; Zhang, C.; Yi, S.; Eddaoudi, M.; Koros, W. J. Mixed matrix formulations with MOF molecular sieving for key energy-intensive separations. *Nat. Mater.* **2018**, *17*, 283−289.

(10) Chuah, C. Y.; Jiang, X.; Goh, K.; Wang, R. Recent progress in mixed-matrix membranes for hydrogen separation. *Membranes* **2021**, *11*, 666.

(11) Dunn, C. A.; Shi, Z.; Zhou, R.; Gin, D. L.; Noble, R. D. (Cross-Linked Poly(Ionic Liquid)−Ionic Liquid−Zeolite) mixed-matrix membranes for CO_2/CH_4 gas separations based on curable ionic liquid prepolymers. *Ind. Eng. Chem. Res.* **2019**, *58*, 4704−4708.

(12) Kamble, A. R.; Patel, C. M.; Murthy, Z. V. P. A review on the recent advances in mixed matrix membranes for gas separation processes. *Renewable Sustainable Energy Rev.* **2021**, *145*, No. 111062.

(13) Farha, O. K.; Eryazici, I.; Jeong, N. C.; Hauser, B. G.; Wilmer, C. E.; Sarjeant, A. A.; Snurr, R. Q.; Nguyen, S. T.; Yazaydın, A. Ö.; Hupp, J. T. Metal−organic framework materials with ultrahigh surface areas: Is the sky the limit? *J. Am. Chem. Soc.* **2012**, *134*, 15016−15021.

(14) Waller, P. J.; Gándara, F.; Yaghi, O. M. Chemistry of covalent organic frameworks. *Acc. Chem. Res.* **2015**, *48*, 3053−3063.

(15) *The Cambridge Structural Database (CSD), UK.* Available from: https://www.ccdc.cam.ac.uk/CCDCStats/Stats (Date of Access: 1 December 2022).

(16) Ongari, D.; Yakutovich, A. V.; Talirz, L.; Smit, B. Building a consistent and reproducible database for adsorption evaluation in covalent−organic frameworks. *ACS Cent. Sci.* **2019**, *5*, 1663−1675.

(17) Qian, Q.; Asinger, P. A.; Lee, M. J.; Han, G.; Mizrahi Rodriguez, K.; Lin, S.; Benedetti, F. M.; Wu, A. X.; Chi, W. S.; Smith, Z. P. MOF-based membranes for gas separations. *Chem. Rev.* **2020**, *120*, 8161−8266.

(18) Wang, R.; Guo, J.; Xue, J.; Wang, H. Covalent organic framework membranes for efficient chemicals separation. *Small Struct.* **2021**, *2*, No. 2100061.

(19) Yeo, Z. Y.; Chai, S.-P.; Zhu, P. W.; Mohamed, A. R. An overview: synthesis of thin films/membranes of metal organic frameworks and its gas separation performances. *RSC Adv.* **2014**, *4*, 54322−54334.

(20) Chakrabarty, T.; Giri, A. K.; Sarkar, S. Mixed-matrix gas separation membranes for sustainable future: A mini review. *Polym. Adv. Technol.* **2022**, *33*, 1747−1761.

(21) Cheng, Y.; Ying, Y.; Zhai, L.; Liu, G.; Dong, J.; Wang, Y.; Christopher, M. P.; Long, S.; Wang, Y.; Zhao, D. Mixed matrix membranes containing MOF@COF hybrid fillers for efficient CO_2/CH_4 separation. *J. Membr. Sci.* **2019**, *573*, 97−106.

(22) Aydin, S.; Altintas, C.; Keskin, S. High-throughput creening of COF embranes and COF/Polymer MMMs for helium separation and hydrogen urification. *ACS Appl. Mater. Interfaces* **2022**, *14*, 21738−21749.

(23) Zornoza, B.; Seoane, B.; Zamaro, J. M.; Téllez, C.; Coronas, J. Combination of MOFs and zeolites for mixed-matrix membranes. *ChemPhysChem* **2011**, *12*, 2781−2785.

(24) Tanh Jeazet, H. B.; Sorribas, S.; Román-Marín, J. M.; Zornoza, B.; Téllez, C.; Coronas, J.; Janiak, C. Increased selectivity in CO_2/CH_4 separation with mixed-matrix membranes of polysulfone and mixed-MOFs MIL-101(Cr) and ZIF-8. *Eur. J. Inorg. Chem.* **2016**, 4363−4367.

(25) Samarasinghe, S. A. S. C.; Chuah, C. Y.; Yang, Y.; Bae, T.-H. Tailoring CO_2/CH_4 separation properties of mixed-matrix membranes via combined use of two- and three-dimensional metal-organic frameworks. *J. Membr. Sci.* **2018**, *557*, 30−37.

(26) Chung, Y. G.; Haldoupis, E.; Bucior, B. J.; Haranczyk, M.; Lee, S.; Zhang, H.; Vogiatzis, K. D.; Milisavljevic, M.; Ling, S.; Camp, J. S.; Slater, B.; Siepmann, J. I.; Sholl, D. S.; Snurr, R. Q. Advances, updates, and analytics for the Computation-Ready, Experimental Metal−Organic Framework database: CoRE MOF 2019. *J. Chem. Eng. Data* **2019**, *64*, 5985−5998.

(27) Willems, T. F.; Rycroft, C. H.; Kazi, M.; Meza, J. C.; Haranczyk, M. Algorithms and tools for high-throughput geometry-based analysis of crystalline porous materials. *Microporous Mesoporous Mater.* **2012**, *149*, 134−141.

(28) Daglar, H.; Aydin, S.; Keskin, S. MOF-based MMMs breaking the upper bounds of polymers for a large variety of gas separations. *Sep. Purif. Technol.* **2022**, *281*, No. 119811.

(29) Dubbeldam, D.; Calero, S.; Ellis, D. E.; Snurr, R. Q. RASPA: molecular simulation software for adsorption and diffusion in flexible nanoporous materials. *Mol. Simul.* **2016**, *42*, 81−101.
(30) Potoff, J. J.; Siepmann, J. I. Vapor−liquid equilibria of mixtures containing alkanes, carbon dioxide, and nitrogen. *AIChE J.* **2001**, *47*, 1676−1682.
(31) Rappe, A. K.; Casewit, C. J.; Colwell, K. S.; Goddard, W. A., III; Skiff, W. M. UFF, a full periodic table force field for molecular mechanics and molecular dynamics simulations. *J. Am. Chem. Soc.* **1992**, *114*, 10024−10035.
(32) Krishna, R.; van Baten, J. M. In silico screening of zeolite membranes for CO_2 capture. *J. Membr. Sci.* **2010**, *360*, 323−333.
(33) Pal, R. Permeation models for mixed matrix membranes. *J. Colloid Interface Sci.* **2008**, *317*, 191−198.
(34) Maxwell, J. C.*A treatise on electricity and magnetism: A treatise on electricity and magnetism*; Dover Publications Incorporated: New York, 1954.
(35) Nagai, K.; Higuchi, A.; Nakagawa, T. Gas permeability and stability of poly(1-trimethylsilyl-1-propyne-co-1-phenyl-1-propyne) membranes. *J. Polym. Sci., Part B: Polym. Phys.* **1995**, *33*, 289−298.
(36) Pinnau, I.; Toy, L. G. Gas and vapor transport properties of amorphous perfluorinated copolymer membranes based on 2,2-bistrifluoromethyl-4,5-difluoro-1,3-dioxole/tetrafluoroethylene. *J. Membr. Sci.* **1996**, *109*, 125−133.
(37) Budd, P. M.; Msayib, K. J.; Tattershall, C. E.; Ghanem, B. S.; Reynolds, K. J.; McKeown, N. B.; Fritsch, D. Gas separation membranes from polymers of intrinsic microporosity. *J. Membr. Sci.* **2005**, *251*, 263−269.
(38) Johnson, T.; Thomas, S. Nitrogen/oxygen permeability of natural rubber, epoxidised natural rubber and natural rubber/epoxidised natural rubber blends. *Polymer* **1999**, *40*, 3223−3228.
(39) Yilmaz, G.; Keskin, S. Molecular modeling of MOF and ZIF-filled MMMs for CO_2/N_2 separations. *J. Membr. Sci.* **2014**, *454*, 407−417.
(40) Ethiraj, J.; Albanese, E.; Civalleri, B.; Vitillo, J. G.; Bonino, F.; Chavan, S.; Shearer, G. C.; Lillerud, K. P.; Bordiga, S. Carbon dioxide adsorption in amine-functionalized mixed-ligand metal−organic frameworks of UiO-66 topology. *ChemSusChem* **2014**, *7*, 3382−3388.
(41) Vitillo, J. G.; Savonnet, M.; Ricchiardi, G.; Bordiga, S. Tailoring metal−organic frameworks for CO_2 capture: The amino effect. *ChemSusChem* **2011**, *4*, 1281−1290.
(42) Habib, N.; Shamair, Z.; Tara, N.; Nizami, A.-S.; Akhtar, F. H.; Ahmad, N. M.; Gilani, M. A.; Bilad, M. R.; Khan, A. L. Development of highly permeable and selective mixed matrix membranes based on Pebax®1657 and NOTT-300 for CO_2 capture. *Sep. Purif. Technol.* **2020**, *234*, No. 116101.
(43) Sabetghadam, A.; Seoane, B.; Keskin, D.; Duim, N.; Rodenas, T.; Shahid, S.; Sorribas, S.; Guillouzer, C. L.; Clet, G.; Tellez, C.; et al. Metal organic framework rystals in mixed-matrix membranes: Impact of the filler morphology on the gas separation performance. *Adv. Funct. Mater.* **2016**, *26*, 3154−3163.
(44) García, M. G.; Marchese, J.; Ochoa, N. A. Effect of the particle size and particle agglomeration on composite membrane performance. *J. Appl. Polym. Sci.* **2010**, *118*, 2417−2424.
(45) Comesaña-Gándara, B.; Chen, J.; Bezzu, C. G.; Carta, M.; Rose, I.; Ferrari, M.-C.; Esposito, E.; Fuoco, A.; Jansen, J. C.; McKeown, N. B. Redefining the Robeson upper bounds for CO_2/CH_4 and CO_2/N_2 separations using a series of ultrapermeable benzotriptycene-based polymers of intrinsic microporosity. *Energy Environ. Sci.* **2019**, *12*, 2733−2740.
(46) Swaidan, R.; Ghanem, B.; Pinnau, I. Fine-tuned intrinsically ultramicroporous polymers redefine the permeability/selectivity upper bounds of membrane-Based air and hydrogen separations. *ACS Macro Lett.* **2015**, *4*, 947−951.

Recommended by ACS

Challenges in Developing MOF-Based Membranes for Gas Separation
Dun-Yen Kang and Jong Suk Lee
FEBRUARY 19, 2023
LANGMUIR READ

Molecularly Homogenized Composite Membranes Containing Solvent-Soluble Metallocavitands for CO_2/CH_4 Separation
Tongxin Liu, Jian-Rong Li, *et al.*
SEPTEMBER 27, 2022
ACS SUSTAINABLE CHEMISTRY & ENGINEERING READ

CO_2/CH_4 Separation via Carbon-Based Membrane: The Dynamic Role of Gas–Membrane Interface
Shanshan Wang, Xiaohua Lu, *et al.*
SEPTEMBER 07, 2022
LANGMUIR READ

Low-Temperature $H_2S/CO_2/CH_4$ Separation in Mixed-Matrix Membranes Containing MFU-4
Qihui Qian, Zachary P. Smith, *et al.*
SEPTEMBER 02, 2021
CHEMISTRY OF MATERIALS READ

Get More Suggestions >

https://doi.org/10.1021/acs.iecr.2c04500
Ind. Eng. Chem. Res. 2023, 62, 2924−2936